The Astrophysical Journal, 652:666–680, 2006 November 20

CHARACTERIZATION OF DUST SHELL DYNAMICS AND ASYMMETRY FOR SIX MIRA-TYPE STARS

K. Tatebe, A. A. Chandler, D. D. S. Hale, and C. H. Townes
Space Sciences Laboratory and Department of Physics, University of California, Berkeley, CA 94720;
tatebe@ssl.berkeley.edu, chandler@ssl.berkeley.edu, david@isi.mtwilson.edu, cht@ssl.berkeley.edu
Received 2006 April 18; accepted 2006 June 28

ABSTRACT

Interferometric observations of six Mira-type stars: R Aqr, CIT 3, χ Cyg, W Aql, R Leo, and U Ori are reported. All measurements were made by UC Berkeley's Infrared Spatial Interferometer (ISI), which is comprised of three 1.65 m telescopes using a heterodyne detection system currently operating at 11.15 μm. All data were taken in a nonredundant east-west linear configuration of telescopes, at a variety of spatial frequencies, with baselines of up to 12 m. By fitting a smooth curve to the closure phase data, as a function of the shortest baseline, the phases of individual visibility measurements can be determined. With curves of the visibility and phase, one-dimensional images are then constructed by an inverse Fourier transform. These images show significant changes in the stars and surrounding dust between the years 2003 and 2004 indicating nonconstant gas emission. They also show significant and varied types of asymmetry, including asymmetries that may be caused by companions, asymmetric stars, or asymmetric dust emission.

Subject headings: circumstellar matter — infrared: stars — stars: variables: other — stars: winds, outflows

1. INTRODUCTION

Mira-type asymptotic giant branch (AGB) stars are characteristically cool, and their low effective temperatures (2000–3000 K) allow a rich molecular composition of their atmospheres. These stars are long-period variables (LPVs) and pulsate with a period on the order of 1 yr. Miras have high mass-loss rates, on average about $10^{-7}\ M_{\odot}\ \mathrm{yr}^{-1}$, which lead to the accumulation of dust in shells around the stars. The relatively large size of the dust shells makes these stars particularly bright at 11.15 μm. The extended atmospheres and energetic pulsations of the Miras also make the existence of asymmetries in the circumstellar material, and perhaps the stars, a likely possibility. Measurements in the mid-infrared are particularly useful as the relatively cool dust can be directly observed in this band and the wavelengths are long enough to be reasonably well transmitted through the dust. Miras are excellent candidates for the study of dust production, motion, and asymmetries in the circumstellar environment using mid-infrared interferometry.

All measurements were made using the University of California, Berkeley, Infrared Spatial Interferometer (ISI) located at the Mount Wilson Observatory in southern California. The ISI consists of three 1.65 m telescopes currently in a linear east-west configuration and uses heterodyne detection with laser local oscillators. The three telescopes allow both visibility and closure phase data to be taken (Hale et al. 2003). Historically, the dust emission has generally been assumed to be spherically symmetric due to sparse Fourier plane coverage and lack of phase information for the fringes observed by interferometry. The ISI's three telescopes now allow measurement of phase closure and more complete visibility curves over relatively short times. However, detailed analysis of interferometrically measured structure is still subject to many complications. The Fourier plane (hereafter referred to as the u-v plane, as u and v are the customary coordinates used to map Fourier space) is only partly covered and only closure-phase information is available, rather than the phases associated with individual visibilities. We attempt to minimize the impact of these limitations by reconstructing stellar images in only one dimension.

We report data on six different Mira-type stars: R Aqr, CIT 3, χ Cyg, W Aql, R Leo, and U Ori using the ISI in a three-telescope linear array. Each of these show emission that can be seen to change with time. These stars, with the exception of CIT 3, have been observed by the ISI previously with two telescopes by Danchi et al. (1994), along with several other stars. ISI observations of CIT 3 have been reported by Lipman et al. (2000) and also by Tevousjan et al . (2004). Data from previous observations, combined with more recent ones, indicate that these late-type stars undergo changes in brightness and dust shell distribution over a decade that are easily observable. Shorter term changes are apparent over 1 yr time spans in more recent data.

2. OBSERVATIONS

The ISI is a three-element, interferometer with 1.65 m apertures. The aperture size was chosen such that the telescope could fit in a standard semitrailer for ease in baseline changes. The ISI was in a linear, east-west configuration with baselines of 4, 8, and 12 m for the measurements presented in this paper. The baselines are labeled as (1-2), (2-3), and (3-1), respectively, with the baseline connecting telescopes 3 and 1 measured from west to east, thus forming a closed "triangle." It is capable of operating at frequencies ranging from 9 to 12 μm; however, all of the data presented in this paper were taken at 11.15 μm in a narrow spectral width of about $\pm$2.6 GHz. A wavelength of 11.15 μm was selected to avoid spectral lines.

The ISI measures both visibility and phase for each baseline. Atmospheric fluctuations distort the phase information for an individual baseline to a degree that renders it unusable for Fourier analysis. This problem is resolved by adding the phase information for all three baselines together. The result is closure phase, a scientifically useful quantity that is not distorted by fluctuations in the atmosphere (Baldwin et al. 1986). The earlier, two-element system is described in Hale et al. (2000), with the update to the three-element array, capable of measuring closure phase, described in Hale et al. (2004). A heterodyne detection system is used where the three local CO_2 lasers are phase locked to a common master oscillator but separated in frequency such that, as the star travels across the sky, fringes are generated at 86, 107, and

TABLE 1
Position Angle Data

Star	Year	Minimum	Maximum	Mean	Spread
R Aqr	2003	77.5	93.8	89.4	16.3
	2004	90.6	109.2	99.1	18.6
CIT 3	2003	85.4	91.7	88.0	6.3
	2004	90.9	95.9	92.5	5.0
χ Cyg	2004	54.0	82.1	68.7	28.1
W Aql	2004	94.3	111.5	101.9	17.2
R Leo	2003	90.6	109.6	98.4	19.0
	2004	91.9	109.2	98.3	17.3
U Ori	2003	107.4	111.4	109.4	4.0
	2004	64.5	114.3	95.5	49.8

Note.—All angles are in degrees east of north for the longest baseline, (3-1).

-193 Hz. When the heterodyned signals from each pair of telescopes are correlated, fringes are produced in Fourier space at each of these three frequencies. By using a master oscillator, the relative phase of each fringe can be preserved, allowing measurement of closure phase, as well as visibility, to be taken.

Data are taken over a variety of spatial frequencies. Over a night of observations, as the altitude of the star varies, the projected baseline on the interferometer changes, giving coverage over a continuous range of spatial frequencies. In the current east-west configuration, the majority of stars measured transit nearly overhead and have only a small rotation angle on the sky, $\lesssim 30^\circ$ (see Table 1). Observation dates of all six stars are given in Table 2.

3. METHODS OF ANALYSIS

3.1. *One-Dimensional Profiles*

Past analysis of ISI data had to assume symmetry in the models, as only one baseline could be recorded at a time (Danchi et al. 1994). The method presented here is able to construct more general images from the data, and with fewer assumptions, since reconstruction is limited to one dimension and phase information is now available. Although the one-dimensional image profile of the dust that is constructed is unique based on the curve fit to the data, it is still subject to sources of error and ambiguity. These include artifacts in the image due to noise in the data, as well as our assumptions of the nature of the visibility and closure phase curves outside the measured range of spatial frequencies.

Closure phase is a useful quantity in determining the qualitative degree of asymmetry of an object. However, to recreate the full image of the star we need the complex visibility, i.e., the visibility magnitude as well as the phase, of the fringe at every point in the u-v plane. The term "visibility phase," here, indicates the phase of the visibility of a single baseline without any added atmospheric effects and should be distinguished from "closure phase," which describes the sum of three such visibility phases around a closed triangle of baselines. In such a sum, the atmospheric effects cancel, leaving the sum insensitive to atmospheric fluctuations. For arbitrary triangular arrangements of the telescopes, there will always be more visibility phases to solve for than there are measured closure phases, precluding direct Fourier inversion. In the present case, however, the linear baseline configuration combined with the continuous spatial frequency coverage over the night allows for an approximate reconstruction of all visibility phases along one axis. We align the x-axis to be along the position angle at which the data was taken. This allows construction of a one-dimensional intensity profile of the source along the axis in question.

TABLE 2
Infrared Spatial Interferometer Observations

Star	Date of Observation	Julian Date (2,400,000+)	Phase[a]	Visible Magnitude
R Aqr	2003 Average	52909	0.09	7.0
	2003 Sep 19	52902	0.07	
	2003 Sep 30	52913	0.10	
	2003 Oct 01	52914	0.10	
	2003 Aug 23	52875	0.00	
R Aqr	2004 Average	53260	0.01	7.5
	2004 Sep 08	53257	0.01	
	2004 Sep 14	53263	0.02	
	2004 Sep 06	53255	0.00	
CIT 3	2003 Average	53908	0.01	...
	2003 Sep 18	52901	0.00	
	2003 Oct 02	52915	0.02	
	1990 Feb 27	47950	0.50	
CIT 3	2004 Average	53286.5	0.59	...
	2004 Oct 07	53286	0.58	
	2004 Oct 08	53287	0.59	
χ Cyg	2004 Average	53246.9	0.25	9.4
	2004 Jul 29	53216	0.18	
	2004 Aug 06	53224	0.20	
	2004 Aug 25	53243	0.24	
	2004 Aug 26	53244	0.24	
	2004 Sep 15	53264	0.29	
	2004 Sep 16	53265	0.30	
	2004 Sep 23	53272	0.31	
	2004 May 17	53143	0.00	
W Aql	2004 Average	53218	0.14	9.7
	2004 Jul 27	53214	0.13	
	2004 Aug 4	53222	0.15	
	2004 May 24	53150	0.00	
	2003 Jan 26	52666	0.00	
R Leo	2003 Average	52973.5	0.19	7.85
	2003 Nov 18	52962	0.15	
	2003 Nov 19	52963	0.16	
	2003 Dec 05	52979	0.21	
	2003 Dec 16	52990	0.24	
	2003 Oct 01	52914	0.00	
R Leo	2004 Average	53336	0.34	8.85
	2004 Nov 19	53329	0.32	
	2004 Dec 03	53343	0.37	
	2004 Aug 10	53228	0.00	
U Ori	2003 Average	52900	0.69	11.6
	2003 Sep 17	52900	0.69	
	2003 Jan 04	52644	0.00	
U Ori	2004 Average	53290.3	1.74	11.1
	2004 Sep 16	53265	1.67	
	2004 Sep 23	53272	1.69	
	2004 Nov 24	53334	1.86	
	2004 Jan 10	53015	1.00	

[a] Phase estimates based on visible photometry provided by AAVSO except for CIT 3, which is taken from Smith et al. (2002). Note that Smith et al. (2002) gives evidence that time lags may exist between visual and IR maxima, although no difference is measured in minima. CIT 3 was calculated from a minima, while all stars based on AAVSO data were calculated from maxima.

To recover the visibility phase at each point, we generate an analytic solution for the phase as a function of the closure phase, assuming all measurements are taken along the x-axis. We assume that both the visibility phase and closure phase are analytic functions and represent them as a sum of polynomial terms:

$$\phi(x) = \sum_{n=0}^{\infty} a_n x^n, \quad \Phi_c(x) = \sum_{m=0}^{\infty} b_m x^m, \tag{1}$$

where $\phi(x)$ and $\Phi_c(x)$ are the visibility and closure phases, respectively, as a function of spatial frequency x.

Thus the equation for closure phase,[1]

$$\Phi_c(x) = \phi(x) + \phi(2x) - \phi(3x), \quad (2)$$

becomes

$$\sum_{m=0}^{\infty} b_m x^m = \sum_{n=0}^{\infty} a_n x^n + \sum_{n=0}^{\infty} a_n (2x)^n - \sum_{n=0}^{\infty} a_n (3x)^n, \quad (3)$$

which can be simplified to

$$\sum_{m=0}^{\infty} b_m x^m = \sum_{n=0}^{\infty} a_n (1 + 2^n - 3^n) x^n. \quad (4)$$

At this point we should note that there is no mixing between monomial terms when creating closure phase from visibility phase. That is, if $\phi(x)$ is purely cubic, then $\Phi_c(x)$ will be as well. Furthermore, were higher terms to be present in $\phi(x)$, they would not alter the coefficients of the cubic term in $\Phi_c(x)$. Hence,

$$b_n x^n = a_n (1 + 2^n - 3^n) x^n, \quad (5)$$

from which we can solve for the phase $\phi(x)$ by solving for $a_n x^n$ and restoring the sums on both sides:

$$\phi(x) = \sum_{n=0}^{\infty} a_n x^n = \sum_{n=0}^{\infty} \frac{b_n x^n}{1 + 2^n - 3^n}. \quad (6)$$

From here, solving for the phase is straightforward. Since the image is real, the phase must be an odd function. Thus, we simply fit a polynomial containing only odd terms, but no linear term,[2] to the closure phase points using the standard least-squares fitting. We then use these coefficients in equation (6) to determine $\phi(x)$. Of course we can only compute the sum to finite order, but in practice only a handful of terms are required to reasonably approximate $\Phi_c(x)$ and thus compute $\phi(x)$. Stated in equation form:

$$\phi(x) \approx \sum_{n=3}^{n_{\max}} \frac{b_n x^n}{1 + 2^n - 3^n}, \quad (7)$$

where $b_n \equiv 0$ for all even n and for $n = 1$.

The visibility phases computed are only valid in the range of spatial frequencies actually measured by any of the baselines, since the closure phase contains no information from outside this range. To account for this, a linear term is first added to the visibility phase curve to make the visibility phase at the highest measured spatial frequency equal to zero. All visibility phases at higher spatial frequencies are then also set equal to zero, as these measurements are assumed to resolve only the symmetric star.

TABLE 3
STELLAR CHARACTERISTICS

Star	Period[a] (days)	Distance (pc)	Stellar Radius (mas)	Flux$_{11\ \mu m}$ 2003 (Jy)	Flux$_{11\ \mu m}$ 2004 (Jy)
R Aqr	387	197[b]	10[c]	1200	1200
CIT 3	660	650[d]	5[e]	1400	1100
χ Cyg	408	106[b]	18[e]	...	1700
W Aql	490	450[f]	11[e]	...	1700
R Leo	310	101[b]	30[g]	2200	1500
U Ori	368	658[b]	10[e]	650	650

[a] Sloan & Price (1998).
[b] *Hipparcos*.
[c] Ragland et al. (2006).
[d] Average value of Hofmann et al. (2001a).
[e] Tevousjan et al. (2004).
[f] Loup et al. (1993).
[g] Weiner (2003).

In addition to phases, we must also obtain the best approximate values of visibility magnitude to have all the data required for an inverse Fourier transform. Since the data must be averaged to achieve a reasonable signal-to-noise ratio, the visibility curve is typically defined by regularly spaced points on each baseline. Despite fairly complete coverage over the range of 2–12 spatial frequency units (SFU),[3] we must interpolate the remaining values in between to form a smooth and continuous visibility curve. We fit a spline curve to the data and convolve the result with a Gaussian to minimize oscillations of the curve due to noise in the data. We also assume a visibility near unity, with the dust not resolved, for all spatial frequencies less than 1/2 SFU. From there the visibility is smoothly brought down to meet the first data point. At the spatial frequencies higher than those measured, we assume the star to be the only significant structure still unresolved. Thus, as a simple approximation, we take the visibility curve at these higher frequencies, up to 2000 SFU, to be that of a uniform disk whose radius is equal to the measured values for each of the stars. Information about the stars' diameters and other properties are given in Table 3. Reported fluxes are based on power measurements relative to α Tauri taken at the ISI during observation.

Two conditions must be met for the method described above to work. First, the closure phase must be a sufficiently smooth function that it can be adequately approximated by a reasonable number of polynomial terms. Second, the object must have a constant position angle over the course of the measurements, so that analysis can be performed in one dimension as assumed in equations (1) and (2).

In practice, neither of these conditions are precisely met. The phase of an image is not constrained to change smoothly and, therefore, neither is the closure phase. Also, virtually every star, except those that transit directly overhead, will have some change in position angle over the course of a night of observing.

In many cases, one can assume these nonconformities to be small, as we will do here. The closure phase is actually measured as an average over a spread of spatial frequencies and is therefore smoothed by the data-taking process. This smoothing, combined with the constraint that the closure phase vanishes at zero spatial

[1] We define x to be the spatial frequency measured by the shortest baseline east to west. For phase closure we must sum the final phase in the reverse direction, from west to east, to form a closed triangle. Since the phase of a real image is an odd function, $\phi(-3x) = -\phi(3x)$.

[2] Linear terms cause divergence of eq (6), but this is of no concern since the addition of a linear component to the phase correlates only to a translation of the image. A linear component is added later to bring the star to the center of the image as a matter of convention.

[3] SFU stands for "spatial frequency unit" and is defined as 10^5 cycles radian^{-1} or, roughly, 0.5 cycles arcsec^{-1}.

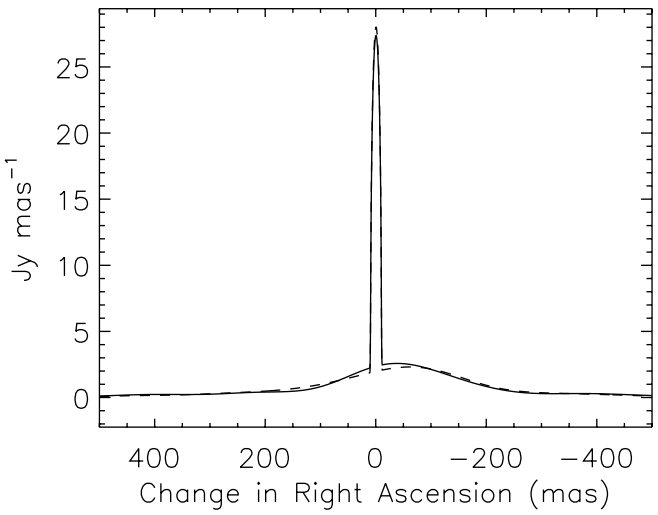

FIG. 1.—Profiles of R Aquarii. The dashed and solid lines are the profiles for 2003 and 2004, respectively. East is to the left.

frequency, allows one to confidently fit a polynomial of a few odd terms to adequately approximate the closure phase. In regards to position angle, many stars will have such a small rotation angle that measurements may be regarded as all being along the same direction on the star.

The tolerance to rotation is given by two quantities: the ratio of the primary mirror diameters to the baseline and how much structure the object has. The rotation of the Earth causes the array to rotate with respect to the star over the night, and in order for the approximation that all data are taken over one position angle to remain valid, this latter rotation should be kept small. If the array rotates only a small amount, then the collection areas of a primary mirror will partially overlap between its old and new orientations. Since most objects observed are unresolved by a single telescope, the wave front of the light is approximately flat over the area of a telescope's primary mirror. Thus, if the array is rotated by a small enough angle, interference fringes are obtained that at least partially represent the same stellar orientation as when the array was in the previous orientation. In this case, the measurement should not be significantly affected. At some point, the array will rotate so far that there will be no correlation between measurements made with the array in the two orientations. When this happens, the one-dimensional approximation may degrade significantly. If the object is relatively smooth and featureless, then the optical wave front incident on the array may be sufficiently flat that there are no significant changes even when the rotation angle is greater than the mirror diameter divided by half of the baseline. In this case, one can extend the one-dimensional approximation to larger changes in position angle.

Given our maximum baseline of 12 m and a mirror diameter of 1.6 m, a rotation of no more than about 16° will provide some correlation between measurements at different position angles. For stars that have somewhat larger rotation angles on the sky, such as R Aqr, the rising and setting data have been measured to be nearly equal, indicating the profile should remain relatively constant over the range of position angles sampled.

The combination of errors in the data, incomplete Fourier coverage, and the complications cited above result in an intensity profile that must be regarded as an approximation, although in many cases a rather accurate and useful one. Most of the information on the dust will be at SFU in the range of 1.5–12, and it is in this range that we will perform analysis and consider results. Despite the smoothness of the profiles, no structure smaller than ~90 mas, equivalent to a half-cycle at our maximum spatial frequency, should be presumed to be well determined.

4. RESULTS

We present results of data taken in the years 2003 and 2004 for six stars: R Aqr, CIT 3, χ Cyg, W Aql, R Leo, and U Ori. Each star is reconstructed using the methods described in § 3. The results are shown in Figures 1–24.

The asymmetries observed may be divided into three general types: (1) Intensity profiles where the lobe of dust is offset from the star's position. It is speculated that these types of asymmetry, found in the cases of R Aqr and CIT 3, may be due to a small companion accreting dust from the primary star. (2) Profiles that show the dust to be unevenly distributed about the star, but with the maximum dust intensity located at or very near the star's position. These cases, found for χ Cyg and W Aql, are suspected to be caused by uneven emission or uneven illumination of the material surrounding the star. This may be caused by the stars themselves being asymmetric, magnetic fields, or simply turbulence. (3) Profiles in which the dust appears to be symmetrically distributed about the star, as in the case of R Leo.

The resolution offered by our longest baseline permits observation of some structure in the profile of intensity emitted by the dust surrounding the star. There is insufficient resolution, however, to determine whether the illumination closely follows any specific curve such as an $R^{1/2}$ behavior. Also, since the particular shape of a star cannot be determined with the resolutions used, a uniform stellar disk is assumed in all cases.

The asymmetry of the dust shells complicates radiative transfer models, making it difficult to derive accurate results. However, for the symmetric source R Leo, we attempted to fit the data using software (see Tevousjan et al. 2004) based on a circularly symmetric model of Wolfire & Cassinelli (1986).

4.1. *R Aquarii*

R Aqr is a symbiotic star system, of spectral type M7 IIIpev, and bright in the mid-infrared. The system consists of a $\sim 1.75\,M_{\odot}$ Mira with a hot subdwarf companion of approximately one solar mass (Hollis et al. 1999). Past ISI measurements of R Aqr can be found in Danchi et al. (1994) and more recently in Tuthill et al. (2000) along with Keck aperture masking data. The profile generated for R Aqr can be seen in Figure 1. The data, taken in 2003 on September 19, 30, and October 1, and in 2004 on September 8 and 9, as well as the associated curves, can be seen in Figures 2 and 3. The visibility phase derived from the closure phase curve is plotted in Figure 4. The χ^2 values for the curves fit to these data, and the data for all other stars presented here, is shown in Table 4.

The profile we have constructed shows the Mira with a lobe of intensity offset to the west (decreasing R. A.) as seen in Figure 1. The Mira is clearly visible in the center of the profile as the high peak corresponding to the profile of a uniform disk. A diameter of ~20 mas is assumed for the star (Ragland et al. 2006).

The offset position of the lobe suggests the symmetry of the dust is broken by some external asymmetry in the system. The companion is the most obvious and probable means of breaking the symmetry of the dust in this way and to the high degree observed. The separation of the Mira and the center of the offset lobe is measured to be 56 and 42 mas in the east-west direction for 2003 and 2004, respectively. These measurements are consistent with an absolute separation of 90 mas with the system oriented roughly 40° from an east-west alignment.

The position angle of the system has been suggested to be around 40° by Hollis et al. (1999) with a separation between the

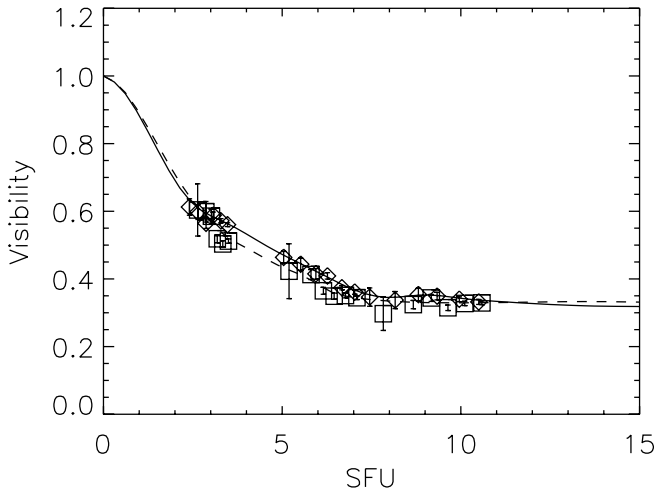

FIG. 2.—Visibility curves of R Aquarii. The dashed and solid lines are the smooth curves fit to the 2003 and 2004 data, respectively. Squares represent data taken in 2003, and diamonds refer to data from 2004.

Mira and companion of approximately 55 mas. This would give an expected separation between the Mira and companion as measured in the east-west direction on the order of 55 mas multiplied by a factor of $\sin 40^\circ$. This would be too small to be consistent with our measurements. There is good reason to doubt the figure of 55 mas based on kinematical considerations. Assuming an orbital period of 44 yr with an eccentricity, e, in the range $0.6 < e < 0.8$ (Hinkle et al. 1989) and with the two stars assumed to have roughly equal masses, we find the separation must be increased for consistency. Calculations by Burgarella et al. (1992) indicate a separation of about 90 mas is required. Further, it is unlikely that our observations would, by happenstance, be taken with the system in an east-west alignment, with the maximum separation of 55 mas in that direction. At a position angle of around 40°, a system separated by 90 mas would appear separated by around 58 mas in the east-west direction. Such a position angle is not entirely inconsistent with past measurements (Hollis et al. 1999; Hege et al. 1991) as the position of the companion is difficult to distinguish from bright areas in the surrounding material. Also, in the 15 yr that have elapsed from these

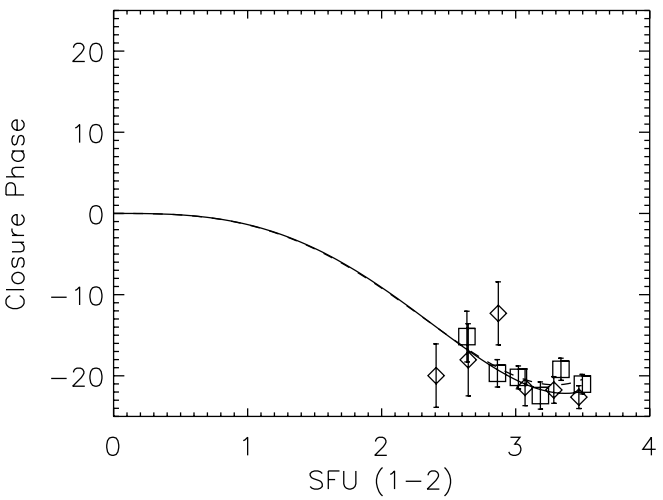

FIG. 3.—Closure phase data for R Aquarii. Curves and symbols follow the same convention as Fig. 2. The dashed curve is difficult to see as it is almost identical to the solid curve up to about 3 SFU, where it begins to turn upward slightly, while the solid curve remains more level. SFU (1-2) values are those of the shortest baseline used.

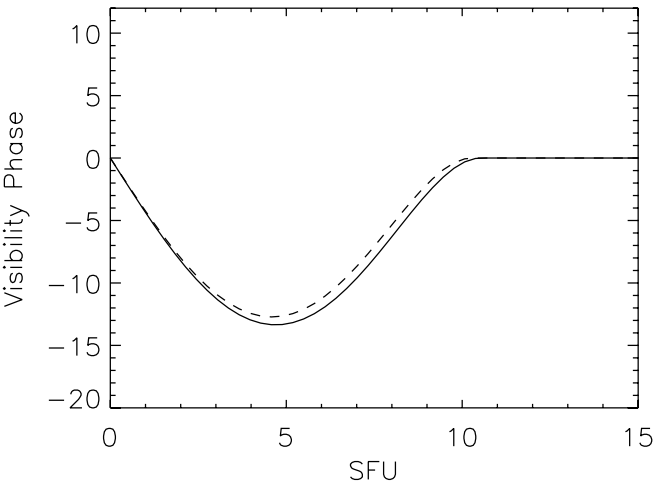

FIG. 4.—Visibility phase curves of R Aquarii. Curves follow the same convention as Fig. 2.

earlier measurements to ours, the system has gone through perhaps a quarter of an orbit and the position angle may have changed appreciably.

The size of the lobe suggests that a large amount of dust is captured by the companion. Parameters for the companion and Mira are given by Burgarella et al. (1992). The companion is stated to have $T_{\rm eff} = 40{,}000$ K, a radius of $\gtrsim 0.1\ R_\odot$, and a luminosity of $10\ L_\odot$. The Mira temperature and radius are 2800 K and $300\ R_\odot$, respectively. A mass-loss rate of $1.3 \times 10^{-8}\ M_\odot\ {\rm yr}^{-1}$ is given by Henney & Dyson (1992). Based on these parameters, the companion is expected to have a bolometric luminosity around half a percent or more of that of the Mira. This means that significant illumination of the offset lobe cannot be from the companion. It seems likely that the lobe represents a somewhat asymmetric dust distribution illuminated by the Mira.

It is striking that the asymmetry in the model so obviously suggests a companion. It is also compelling that the separation between this offset lobe and the Mira is on the order of what one expects from other measurements for the separation of the Mira and the companion. The earlier measurements by Tuthill et al. (2000) in the near-infrared and mid-infrared were unable to detect a companion. The near-infrared closure phases were zero to within errors, although variations in structure with position angle were detected in the mid-infrared.

Given an outflow rate of about 30 km s^{-1} (Kenyon et al. 1988), which at a distance of 200 pc corresponds to 31.4 mas yr^{-1}, the outer reaches of the dust shell would have left the Mira about 20 yr ago. The smoothness of the lobe with few significant features implies an approximately constant outflow over the past

TABLE 4

χ^2 VALUES FOR CURVES FIT TO DATA

Star	Year	$\chi^2_{\rm vis}$	$\chi^2_{\rm CP}$
R Aqr	2003	1.98	0.84
	2004	1.24	1.48
CIT 3	2003	6.65	1.22
	2004	0.82	0.11
χ Cyg	2004	1.04	0.04
W Aql	2004	1.45	0.53
R Leo	2003	8.54	0.60
	2004	2.00	0.22
U Ori	2003	0.37	0.72
	2004	1.38	23.09

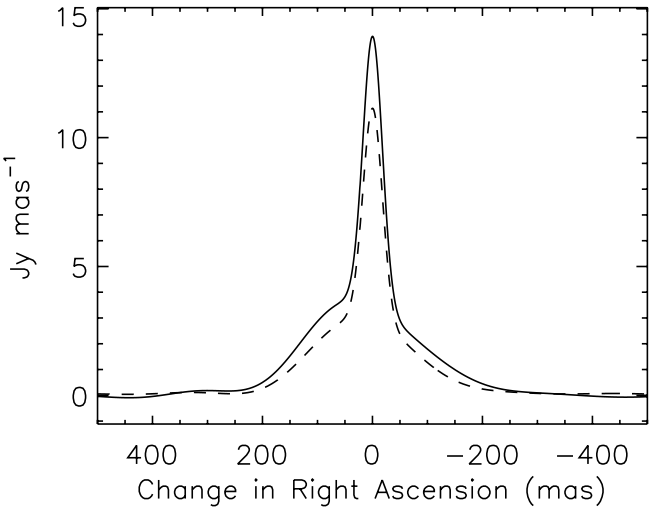

FIG. 5.—Profiles of CIT 3. The dashed and solid lines are the profiles for 2003 and 2004, respectively.

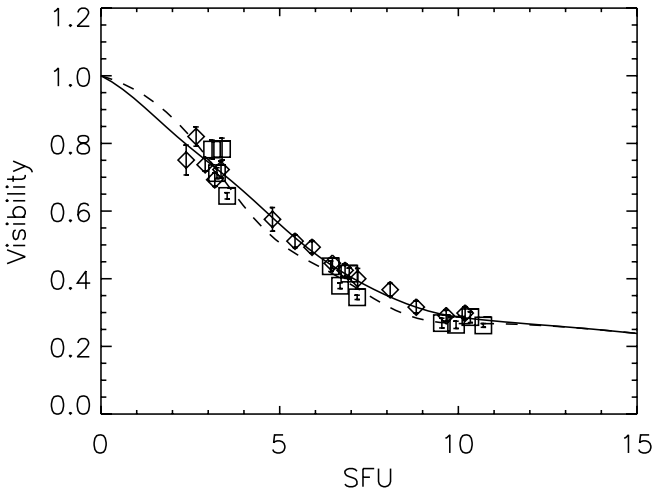

FIG. 6.—Visibility curves of CIT 3. The dashed and solid lines are the smooth curves fitted to the 2003 and 2004 data, respectively. Squares represent data taken in 2003, and diamonds refer to data from 2004.

16 yr with no strong variations. This is consistent with a long orbital period for the companion. The surrounding dust produces flux on both sides of the Mira and slowly fades to zero from about 300 to 500 mas from the star. Past ISI measurements of this star, Danchi et al. (1994) and Tuthill et al . (2000), show that the total amount of dust surrounding the star has remained rather constant over the last 25 yr, with visibility of the star itself near 0.25.

The companion is strongly expected to accrete significant material (Hollis et al. 1999) and jets detected in the radio, visible, ultraviolet, and X-ray are most easily accounted for by accretion (Kellog et al. 2001; Hollis et al. 1997). At closest approach the dwarf is believed to be within the Roche lobe of the Mira, and this likely leads to substantial accretion of the mass outflow, perhaps around 10%, from the Mira onto the dwarf companion (Michalitsianos et al. 1998). The present measured separation implies that the system is currently at or near periastron with a significant amount of material offset from the Mira's position. Accretion is expected to occur primarily near closest approach, when the companion is perhaps within the Mira's Roche lobe. Absorption of the material by the companion probably takes longer than its orbital period about the Mira, so it remains surrounded by dust even at its present, relatively large, separation.

The visibility and closure phase curves for 2003 and 2004 show the object to have similar overall character at all of the measured spatial frequencies, and the qualitative shape of the images remain comparable. The total flux is also the same for each epoch as one might expect since both are approximately at the same phase, as seen in Table 2. The virtually identical character of the curves indicates that there has been no significant change in the distribution, or quantity, of dust surrounding the star. This is consistent with the rather constant visibility curves measured at the ISI over the past several years for R Aqr (Danchi et al. 1994). If the companion is responsible for the dust asymmetry, its orbital period must be long enough to produce no significant changes in the dust distribution over 1 yr. This is also consistent with present estimates of a relatively long orbital period for the companion.

4.2. *CIT 3*

CIT 3 is an M9 spectral type LPV that shows the beginnings of asymmetry (Hofmann et al. 2001a) and a large amount of accumulated circumstellar material (Vinkovic et al. 2004). We report on CIT 3 based on data taken in 2003 on September 18 and October 2 and in 2004 on October 7 and 8. The profile, seen with associated plots in Figures 5–8 of CIT 3, displays a clear asymmetry and bears a striking resemblance to R Aqr, with a central peak of intensity and an offset lobe of dust. This resemblence is even more apparent if the central peak is made more narrow and suggests, as in the case of R Aqr, that a companion may be the source of the asymmetry. Jura & Kanane (1999) have also proposed that a binary companion would be a logical means to explain the bipolar outflows observed by Vinkovic et al. (2004). Other explanations, however, may be able to account for the asymmetry without the need for a companion. Hofmann et al. (2001a) suggest that CIT 3 is just entering the final portion of the AGB phase, where asymmetries are expected to begin as it transitions to a planetary nebula.

If there is a companion, it must pass within the Roche lobe of the Mira for significant accretion to occur. Since the asymmetry is relatively unchanged between the two epochs, the orbital period must be much greater than a few years. For the companion to both come within the Roche lobe of the Mira and have a long orbital period, the orbit must be highly eccentric. Furthermore, the fact that flux from the dust seems to track the stellar phase, and in rough proportion to the stellar luminosity, reinforces the conclusion that the illumination of the dust is mainly due to radiation from the Mira. This is similar to the observed character of R Aqr and indicates that an unseen companion would be something much less luminous that the Mira, such as a dwarf-like star.

Unlike the other stars presented here, a Gaussian rather than a uniform disk fit is used to complete the visibility curve at high spatial frequencies. This is done to remain consistent with previous visibility measurements that show the object to be almost completely resolved at higher spatial frequencies (Lipman et al. 2000). Also, SED fitting shows that virtually all of the flux should come from the dust surrounding the star (Hofmann et al. 2001a). Furthermore, models fit to past ISI data by Lipman et al. (2000) indicate that the star is too small to generate the flux required ($\sim$50 Jy mas^{-1}) for a uniform disk consistent with the measured high-frequency visibilities and assumed stellar radius. These past models also indicate that the optical depth of the dust is greater than unity, thus preventing the disk of the star from being clearly distinguished from the dust.

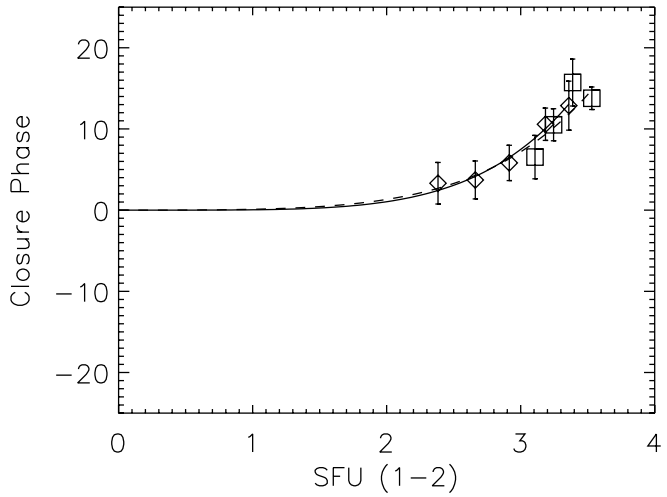

FIG. 7.—Closure phase data for CIT 3. Curves and symbols follow the same convention as Fig. 6.

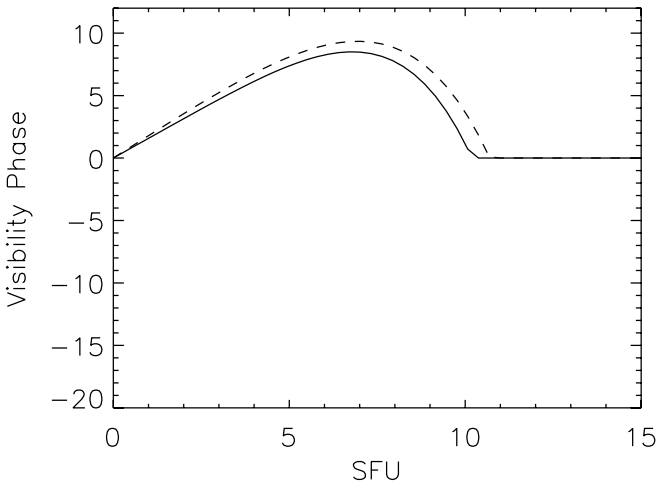

FIG. 8.—Visibility phase curves of CIT 3. Curves follow the same convention as Fig. 6.

The flux difference at the two epochs is difficult to determine with the calibration data available. The two epochs are near minimum and maximum phase and should show a significant change in flux at 11.15 μm. Estimated fluxes are approximately 1400 and 1100 Jy for the 2003 and 2004 data, respectively. However, Lipman et al. (2000) give the flux as 1350 Jy at $\phi = 0.65$, indicating our estimates may be somewhat low. The visibility and closure phase curves are similar in 2003 and 2004 but show a slight decrease in the broadness of the dust distribution, most easily recognized by the more resolved 2003 visibility curve. This is most likely due to changes in illumination with stellar phase, and changes in the distribution of dust are probably small.

Many measurements to help characterize the size and configuration of the star and surrounding material have been made. Flux in the profile falls to near zero at a distance of approximately 200 mas. This is roughly one-third the maximum possible size estimated by Sudol et al. (1999) but is in fair agreement with earlier ISI measurements indicating a dust shell no larger than 630 mas (Lipman et al. 2000). Present visibilities are somewhat higher than those measured in 2000 and are consistent with the flux from the dust shell being somewhat smaller now, perhaps due to the dust expanding and becoming more diffuse. An outflow velocity of 23 km s^{-1} (Knapp & Morris 1985) corresponds to an angular expansion of 7.4 mas yr^{-1} at a distance of 650 pc. This would give an expansion of just over 40 mas between the present measurements and those of Lipman et al. (2000). Measurements at 8.55 μm show elongation along a position angle of -14° fit by a two-dimensional Gaussian with a cross-sectional eccentricity of 0.31 (Marengo et al. 1999). Observations from CO emissions by Neri et al. (1998) give an elongation at a position angle of around -45°, as fit by Marengo et al. (1999).

Near-infrared measurements using aperture masking on the Keck telescope, as described by Tuthill et al. (1998), showed no significant deviations from axial symmetry. Present ISI observations, however, show that there are significant differences in the distribution of material on the two sides of the star. The present visibility curves also differ from those of Lipman et al. (2000) in that they are about 10% lower.

The asymmetry of CIT 3 has been imaged in the *J* band by Hofmann et al. (2001a) as a fanlike structure pointing to the northwest between position angles -8° and -48°, opposite to the direction of the asymmetric structure we detect. Other measurements in the near-infrared have shown indications of a bipolar structure as close as 100 mas from the star (Vinkovic et al. 2004). The asymmetry at 10 μm does not appear to be that of a fanlike structure and it is likely that the fanlike asymmetry found in the *J* band is not present in the *N* band.

4.3. χ *Cygni*

χ Cyg is an S-type star that has a dust distribution whose intensity peaks near the star but is not in a symmetric distribution on the two sides of the star. The falloff in intensity of the dust to the east is much more gradual than to the west. This indicates that there may be a steady excess of dust emitted to the east. Alternatively, there may be a current hot spot on the east side of the star that illuminates a symmetric dust shell in an asymmetric way. Despite the more rapid initial rate of falloff in intensity close to the star on the west side, the intensity appears to persist at low levels farther out. The point at which the intensity falls to near zero is about the same distance from the star to either side, about 350 mas.

The peak of the dust intensity is not more than slightly offset from the star's center, indicating a different sort of asymmetry than the kind observed in the cases of R Aqr and CIT 3. This indicates that a companion is unlikely to be the source of asymmetry in this case. Groenewegen (1996) suggests the asymmetry in the dust may be due to an aspherical shape of the Mira but also claims χ Cyg possesses a companion. Tuthill et al. (1999) have reported departures from spherical symmetry of the photospheric surface of χ Cyg. Departures from spherical symmetry, particularly in the photosphere, could account for the uneven illumination of the material surrounding the star and the resulting apparent asymmetry in the dust. A simple oblate shape, however, would not account for the asymmetry we observe. Rather, the star would be need to be brighter on one side than the other to produce asymmetries that yield a nonzero closure phase measurement.

Young et al. (2000) report no asymmetry in the visible and that a Gaussian star shape fits their data better than a uniform disk. They attribute this to a very extended stellar atmosphere, one in which turbulent effects may play an important role. Such effects may increase the size of the star and its fluctuations. The case for convection and perhaps other turbulent atmospheric conditions is also supported by the presence of heavier elements, such as technium, in its atmosphere (Wang & Chen 2002). Turbulent effects in the atmosphere may couple with the regular pulsation of the Mira to produce uneven illumination.

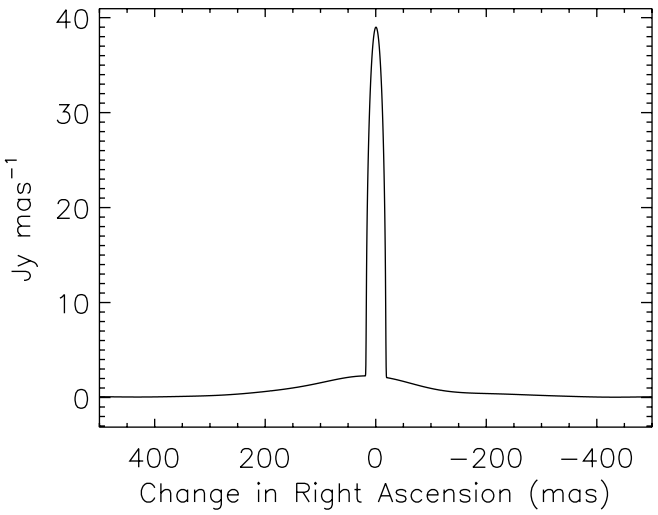

FIG. 9.—Profile of χ Cygni for 2004.

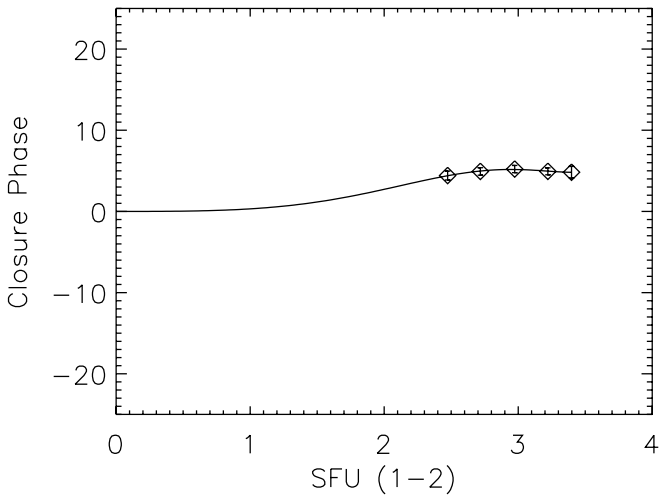

FIG. 11.—Closure phase data for χ Cygni. Symbols follow the same convention as Fig. 10.

Previous ISI measurements of the visibility curve of χ Cyg have been reported by Danchi et al. (1994) and Tevousjan et al. (2004) and are in good agreement with Sudol et al. (1999). Present measurements, taken in 2004 on July 29, August 6, 25, 26, September 15, 16, and 23, are not exceptionally different, although we find χ Cyg to have somewhat higher visibilities at lower spatial frequencies than Sudol et al. (1999). The profile and associated data for χ Cyg are shown in Figures 9–12. Lack of closure phase data for previous measurements allows no conclusions about how the asymmetry may have developed with time. The visibility curve, however, has changed significantly since it was reported on by Danchi et al. (1994). The previous measurements show χ Cyg to be more resolved in the 1992 measurements, taken at a phase of 0.35, and significantly more resolved at low spatial frequencies in 1988, taken at a phase of 0.88. The change in the visibility curve from the 1992 measurements to those reported here can probably be accounted for by the change in stellar phase. The more dramatic difference, at low spatial frequencies, between the 1988 and present data indicate that significant changes in the structure of the dust surrounding the star have occurred.

The uneven but smooth intensity distributions to either side of the Mira allow uneven illumination, uneven outflow, or a companion to be possible explanations. The relatively small amount of dust surrounding the star makes discerning the effect of a companion difficult, but the lack of a distinct maximum in the dust intensity offset from the star and lack of evidence for a binary that has a close orbit to the Mira suggest that this is not the most likely scenario. The observed asymmetry may be due to local hot spots on the star due to convection, uneven outflow, or patchy illumination of the outer dust due to shadowing from dust close to the star, rather than the effects of a companion. Soon, the configuration of the ISI will be changed to a triangular configuration with ~30 m baselines in order to resolve stellar asymmetries. In this configuration it will not only be possible to distinguish between spherical and oblate shapes, but asymmetries in flux from different sides of the star, e.g., due to an egglike shape or a hot spot, will also be detectable. These future characterizations of stellar asymmetries will help to determine the origins of the asymmetries currently observed in the material surrounding this and other stars.

4.4. *W Aquilae*

W Aql is a particularly bright star, of spectral type S, on which we have taken data over a wide range of spatial frequencies. The

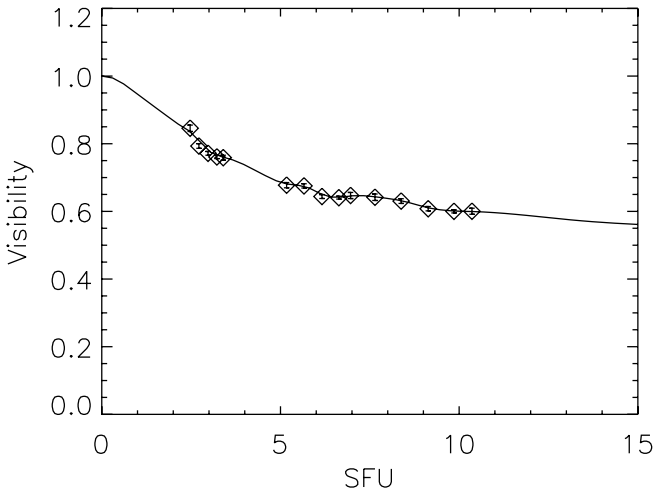

FIG. 10.—Visibility curve of χ Cygni for 2004. Diamonds refer to measured data from 2004.

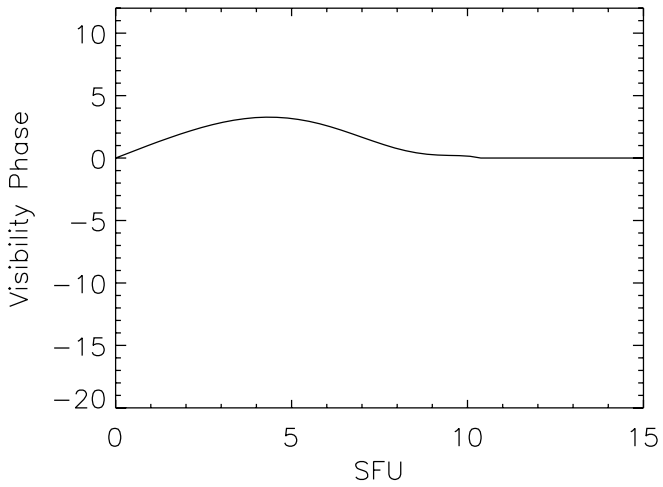

FIG. 12.—Visibility phase curve for χ Cygni.

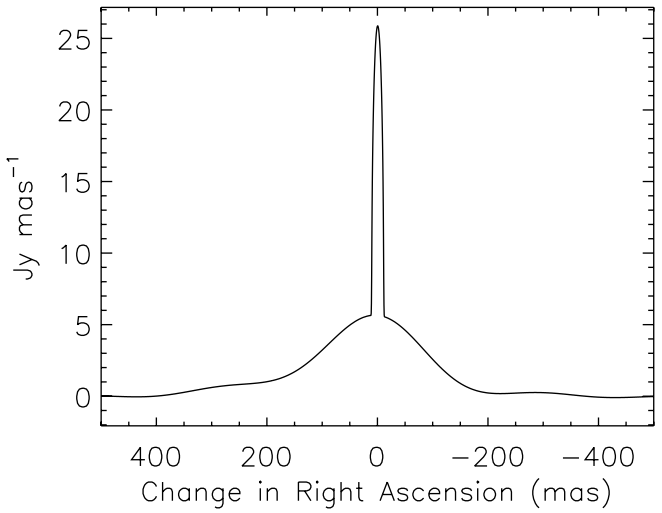

FIG. 13.—Profile of W Aquilae for 2004.

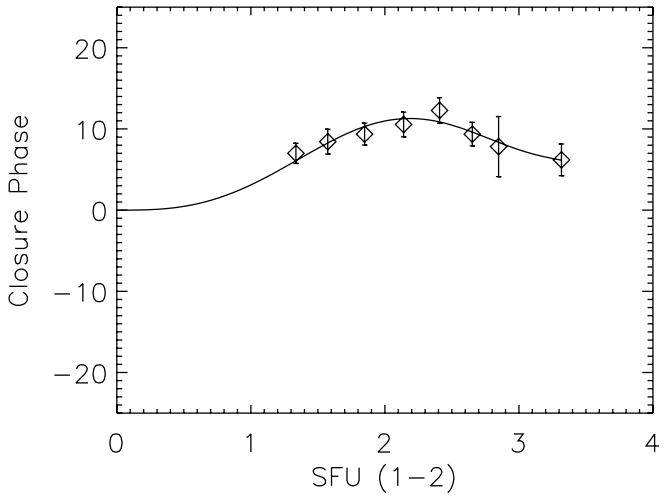

FIG. 15.—Closure phase data for W Aquilae. Symbols follow the same convention as Fig. 14.

small errors, the relatively small change in position angle, and the smooth nature of the visibility and closure phase curves make W Aql an ideal candidate for this type of one-dimensional reconstruction. Data for W Aql are from 2004 on July 27 and August 4. There are no data available from 2003, but previous observations by the ISI were reported by Danchi et al. (1994) and by Tevousjan et al. (2004).

The profile of W Aql along with the associated plots can be seen in Figures 13–16. The profile shows that the peak of intensity from the dust distribution is fairly well aligned with the star, but with an asymmetric distribution of dust much like χ Cyg, although with significantly more dust. There is a clear excess of dust to the east of the star relative to the west side. Also, the falloff in intensity of the dust to the east is more gradual than the dust on the west side. The profile is of a different character than those of R Aqr and CIT 3 where a companion may be indicated. The asymmetry here may be due to asymmetric emission of dust rather than an external effect causing asymmetry in a symmetric outflow. The asymmetry in the outflow of the dust may be due to magnetic effects, which eject material in particular directions, or to convection and turbulence in the atmosphere of the star.

Both the shallow wiggles in the visibility curve and the rises in intensity of the dust profile indicate nonconstant gas emission, e.g., a "dust shell." Given a typical outflow velocity of 20 km s^{-1}, the dust shell was probably emitted sometime within the last 35 yr. The outer as well as the inner dust is more intense on the westward side, indicating that the asymmetry may be stable at least over moderately long time spans. If the asymmetry is indeed stable over periods as long as 35 yr or more, a companion is an unlikely source of asymmetry, as this is the characteristic timescale one might expect for the orbital period of a companion. It is also unclear how a companion would alter the distribution of material over such large distances. In the cases of R Aqr and CIT 3, the peak of the dust is offset but is still rather compact and symmetric. In the cases of χ Cyg and W Aql the asymmetry in the distribution of the dust is apparent even far from the star with consistently more intensity observed on one side of the star at all distances. This might be a constant effect with more material being emitted to the west whenever material is ejected. Alternatively, the emission of dust may be generally symmetric with

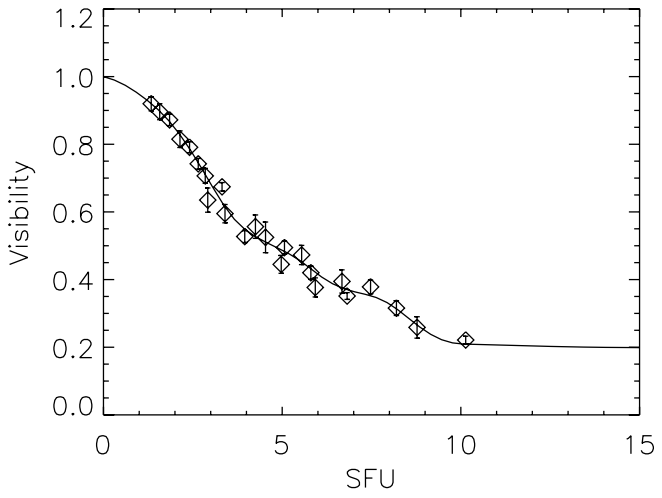

FIG. 14.—Visibility curve of W Aquilae for 2004. Diamonds refer to measured data from 2004.

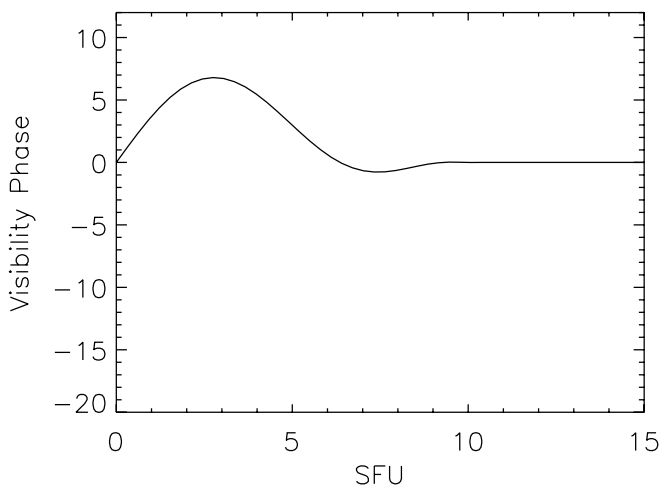

FIG. 16.—Visibility phase curve for W Aquilae.

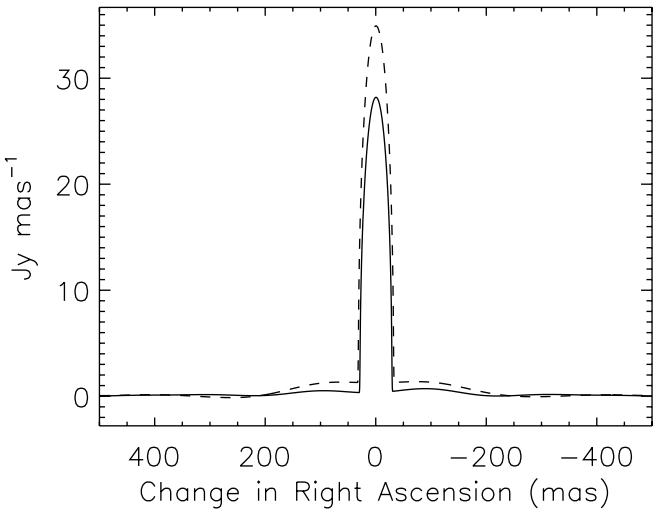

FIG. 17.—Profiles of R Leonis. The dashed and solid lines are the profiles for 2003 and 2004, respectively.

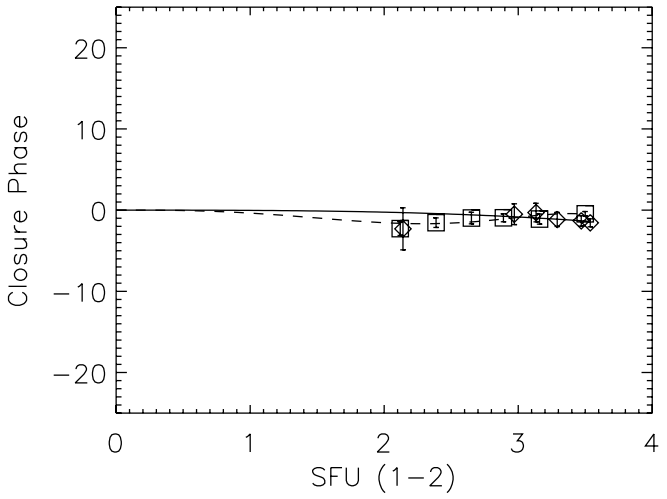

FIG. 19.—Closure phase data for R Leonis. Curves and symbols follow the same convention as Fig. 18.

only intermittent emissions in the westward direction that generated the observed asymmetry.

4.5. *R Leonis*

The M8 IIIe–type Mira variable R Leo is of special importance because it is one of the most luminous Mira variables (in the visible) and therefore is one of the best studied. Data for 2003 were taken on November 18 and 19 and December 5 and 16. Data for 2004 were taken on November 19 and December 3. We assumed diameters of 32 and 29 mas for 2003 and 2004, respectively, by modifying values proposed by Weiner (2003) for the phases at which we measured the star. The profile and associated plots can be seen in Figures 17–20. R Leo is the only star in this sample that was measured at a substantially different phase for the two epochs. The profiles show a dramatic change in the relative dust-to-star intensity, but the structure is fairly unchanged between epochs. The closure phase is very nearly zero over all spatial frequencies, so interpretation of the visibility curve is perhaps simpler than for the stars previously discussed. There are oscillations in the visibility curve that are similar in both epochs, but are somewhat more distinct in the 2003 data.

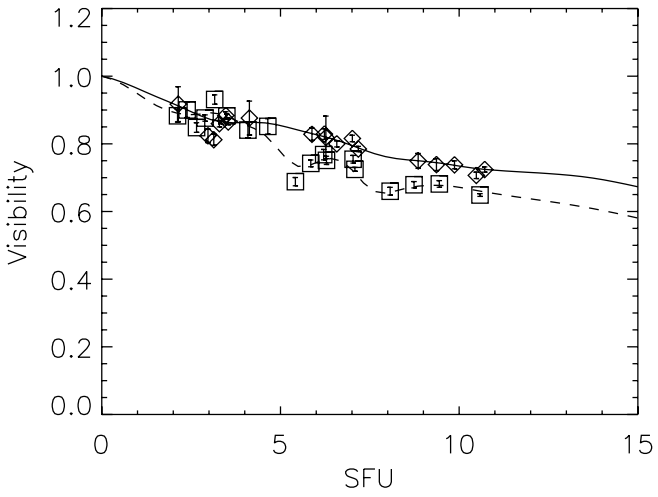

FIG. 18.—Visibility curves of R Leonis. The dashed and solid lines are the smooth curves fit to the 2003 and 2004 data, respectively. Squares represent data taken in 2003, and diamonds refer to data from 2004.

The main difference in the visibility curves is the change in the overall level as a result of the unresolved star contributing proportionally more intensity in the 2004 data. While it is possible for the relative intensities of the star and dust to change counter to one another, the total flux from the dust and star individually can be expected to increase or decrease together. In the case of R Leo, the intensities of the star and dust both decrease from 2003 to 2004, much like CIT 3, while R Aqr remains virtually unchanged.

For both epochs, R Leo was found to be very nearly symmetric. For the first epoch (2003) the closure phase of R Leo did not vary significantly with resolution, being about -0.92° over the dates of our observations. During the second epoch (2004) the closure phase was also constant at about -0.7°. The flux from the dust shell surrounding the star has decreased significantly from 2003 to 2004 and is likely due to the dust being diluted as it flows outward. At a distance of 101 pc, a 25 km s^{-1} outflow rate would shift the dust outward by approximately 50 mas in 1 yr. This is consistent with the changes seen in the dust shell between the two epochs. The dust in the 2004 image, as seen in Figure 17, shows the flux to decrease just beyond the surface of the star. This may mean that dust production has diminished recently and

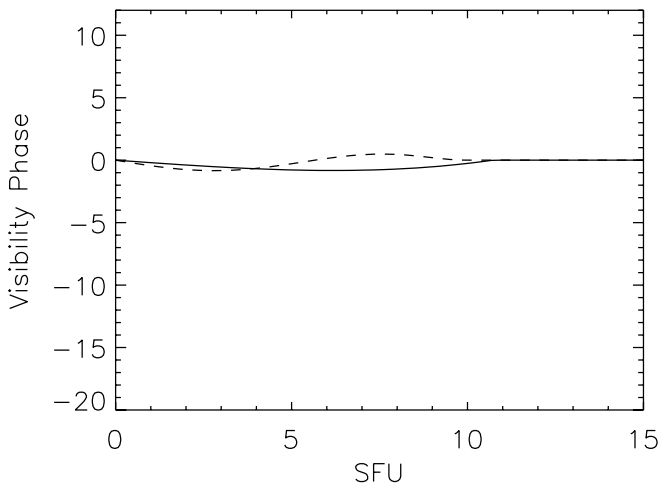

FIG. 20.—Visibility phase curves of R Leonis. Curves follow the same convention as Fig. 18.

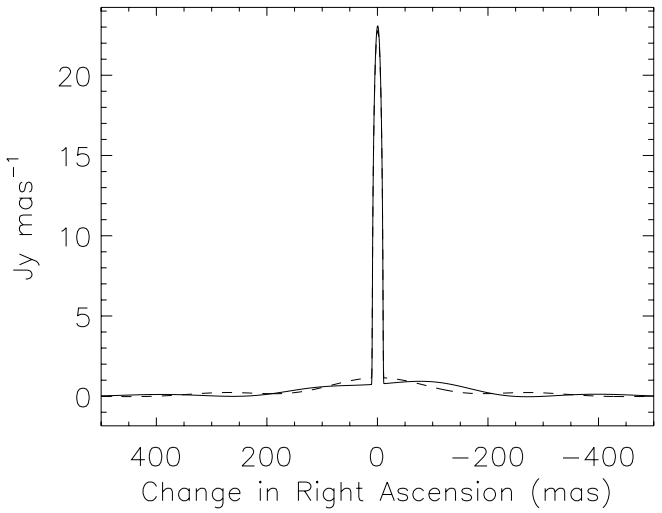

FIG. 21.—Profiles of U Orionis. The dashed and solid lines are the profiles for 2003 and 2004, respectively.

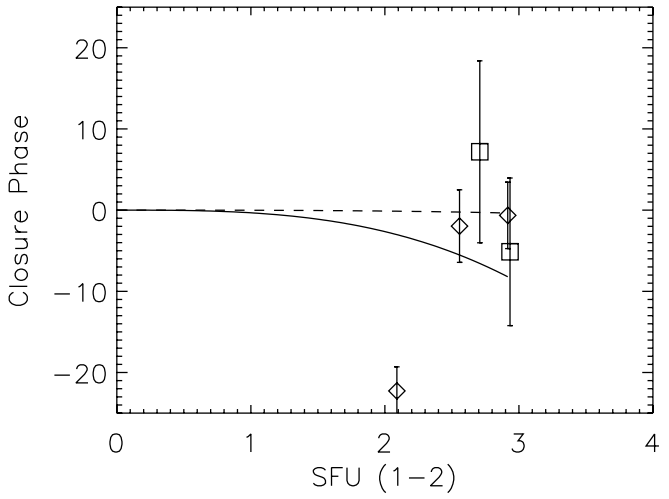

FIG. 23.—Closure phase data for U Orionis. Curves and symbols follow the same convention as Fig. 22.

that the small lobes of intensity to either side of the star may be due to the still expanding shell of dust surrounding the star. The greater flux from dust surrounding R Leo in 2003 shown in Figure 17 results from the more resolved, i.e., lower, visibility curve seen in Figure 18, where the visibility falls significantly beyond 4 SFU.

Since we find R Leo to be symmetric, we also modeled it using the algorithm by Wolfire & Cassinelli (1986). The model, with parameters such as the stellar temperature and diameter, inner radius of dust formation, and dust composition, was used to fit both the measured visibility curve and a spectral curve. No reasonable model could be found that fit both curves. Models that most closely approximated the curves required a star temperature of 900 K, indicating that a good fit was not possible. This may be due to the star, and perhaps the dust, having an oblate shape. This shape would invalidate the assumptions of spherical symmetry made by the algorithm but would not be indicated by our measurements along only one position angle. The program is also incapable of modeling multiple dust shells around the star.

Despite being well studied, R Leo is still not well understood. Although we do not report any significant asymmetry of the dust, asymmetry in the star itself has been detected in the visible with the *Hubble Space Telescope* (Lattanzi et al. 1997) and with other interferometric methods (Tuthill et al. 1999). Some research suggests that simple symmetric models like uniform disk fits and basic shell models do not accurately represent the data (Danchi et al. 1994; Schuller et al. 2004). Other measurements in the visible and near-infrared regime found R Leo to be symmetric (Hofmann et al. 2001b). The dense dust shells around this type of AGB star make results in the visible uncertain due to the obscuring effects of the dust, which may include uneven limb darkening. The 11.15 μm measurements reported here suggest that the dust is emitted in a symmetric distribution.

4.6. *U Orionis*

U Ori is an oxygen-rich M8 III–type Mira variable. We report that asymmetry based on closure phase measurements is detected at low spatial frequencies in the 2004 data, taken on September 16, 23, and November 24, although none was detected, to within errors, in the 2003 data taken on September 17. These data and the associated curves and image profile can be seen in Figures 21–24. There are some apparent changes in the visibility curve between the two epochs in the middle of our

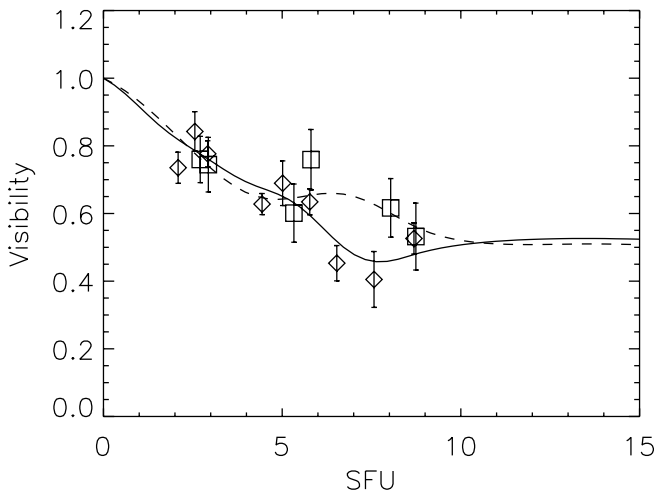

FIG. 22.—Visibility curves of U Orionis. The dashed and solid lines are the smooth curves fit to the 2003 and 2004 data, respectively. Squares represent data taken in 2003, and diamonds refer to data from 2004.

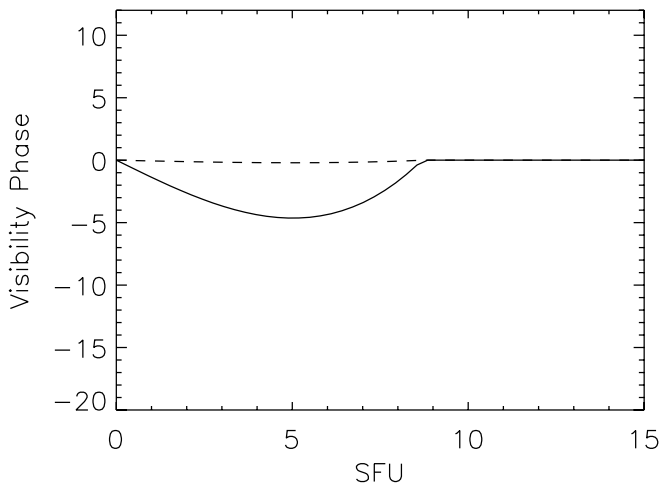

FIG. 24.—Visibility phase curves of U Orionis. Curves follow the same convention as Fig. 22.

TABLE 5
Visibility and Closure Phase Calibration Errors

Date	Baseline (%) (1–2)	(2–3)	(3–1)	Closure Phase (deg)
2004 Jul–Aug	3.5	3.3	3.9	1.1
2004 Sep–Oct	1.8	1.1	1.2	1.1
2004 Nov–Dec	2.1	1.4	3.3	1.1
2005 Nov–Dec	1.6	1.7	3.2	0.7

measured spatial frequency range, indicating a possible change in the configuration of the dust surrounding the star. Relatively constant visibilities at the lowest frequencies indicate the dust shell is approximately the same size, and the relative dust-to-star brightness may be relatively unchanged as it is resolved to similar levels at the highest measured frequencies. Since U Ori is a relatively dim, and possibly more distant, star the data have larger uncertainties than those of any other star reported here. Although a distance of 658 pc is stated in Table 3, other measurements indicate the distance may be more than a factor of 2 smaller (Mondal & Chandrasekhar 2004; Haniff et al. 1995; Danchi et al. 1994). Also, as seen in Table 1, the change in position angle of U Ori during observation is considerably larger than for any other star presented here.

The nonzero closure phase in the 2004 data indicates that there may be greater intensity on one side of the object than the other, although the uncertainties may be somewhat greater than those indicated by our error bars, which are based only on the statistical fluctuations of the measurements. The actual values indicated vary depending on what bandwidths we integrate the fringe over and how much averaging of the data is performed. Still, measurements near 2 SFU were consistently below zero well outside of probable errors while all other frequencies were zero to within errors regardless of how the data were processed. The fit shown in Figure 23 for the 2004 data is a cubic fit. Using higher order polynomials in an attempt to fit the closure phase data better produced questionable images with negative intensities.

U Ori has been measured twice by the ISI prior to these reported observations. The first set of observations by Danchi et al. (1994) resulted in a model with a stellar radius of 7.2 mas and an inner dust shell radius of 80 mas. Later observations by Tevousjan et al. (2004) fit the data with an assumed stellar radius

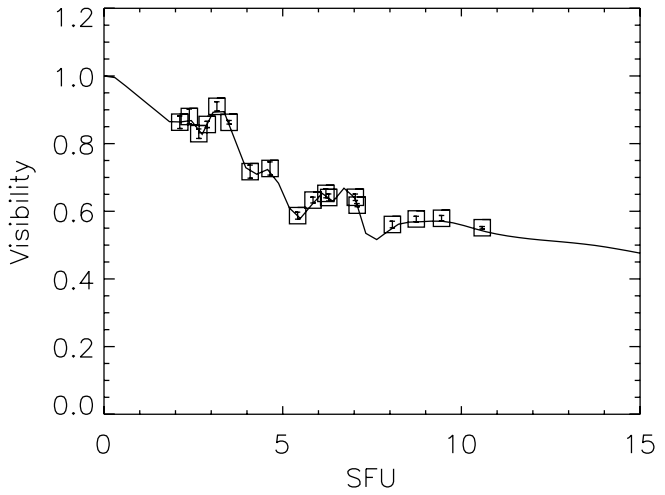

Fig. 26.—Fit to the visibility curve of R Leonis corresponding to the image in Fig. 25.

of 10.75 mas and the inner dust shell radius of 55 mas. Our measurements show the present visibility at 8 SFU to be comparable to that reported by Tevousjan et al. (2004) and perhaps slightly higher than on the curve fit by Danchi et al. (1994).

Other measurements of U Ori consistently show asymmetries in the star or the dust shell. The variation with position angle of uniform disk fits to near-infrared lunar occultation data suggest an elongation in the NE-SW direction at a position angle of $\approx 70^{\circ}$ (Mondal & Chandrasekhar 2004; Richichi & Calamai 2003). Also, VLA observations of OH masers by Bowers & Johnston (1988) find an elongation of the molecular shell containing the masers to the NE. Future ISI measurements at longer baselines may help to confirm these stellar asymmetries.

5. DISCUSSION OF ERRORS

In the one-dimensional images presented, it is important to recognize which structures are likely to be genuine and which may be artifacts. Fairly complete visibility curves are described by the data, and it is possible to fit smooth curves to these data with fairly high confidence, although the calibrations do introduce some errors. Errors in calibration for a given baseline, or closure phase zero, simply move the associated data up or down

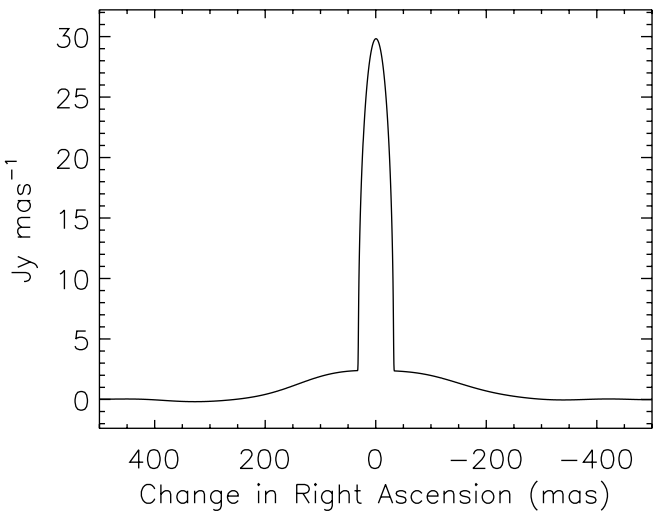

Fig. 25.—Profiles of R Leonis using detailed fit to the data, shown in Figs. 26 and 27.

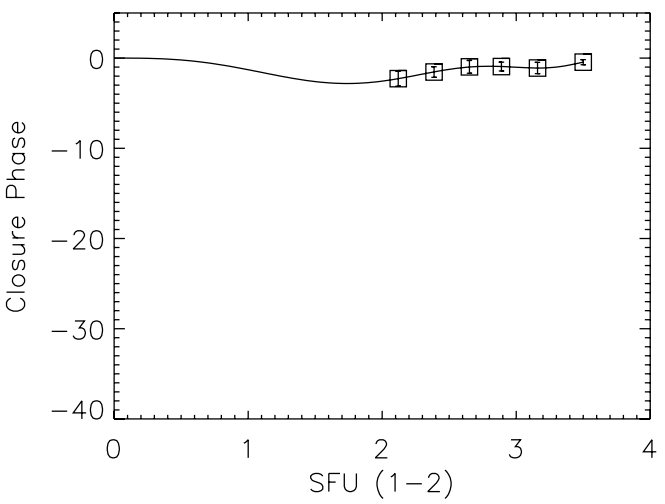

Fig. 27.—Curve fit to the closure phase data of R Leonis corresponding to the image in Fig. 25.

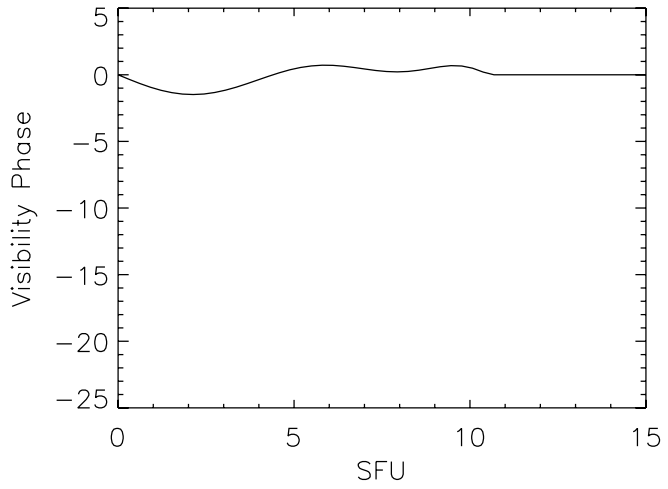

FIG. 28.—Visibility phase curve corresponding to the closure phase fit shown in Fig. 27.

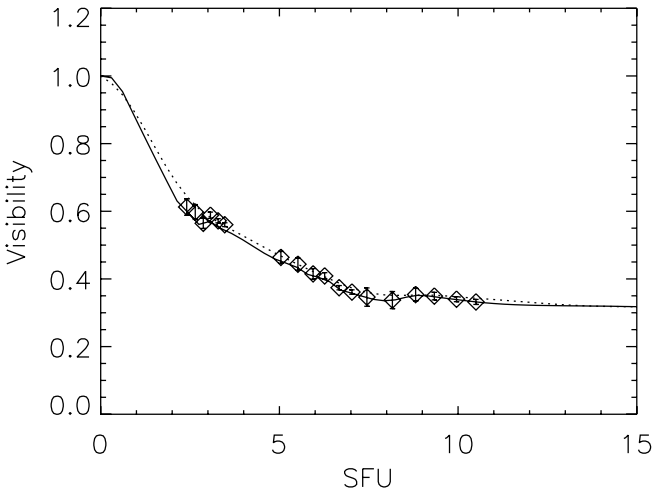

FIG. 30.—Visibility curves for R Aquarii corresponding to the images in Fig. 29.

in the figures presented. A summary of errors due to calibration for the visibility and closure phase are shown in Table 5.

In addition to the data calibrations, the fit visibility curves themselves may be modified, and remain consistent with the data, by introducing more structure (i.e., wiggles) to the curve, or by modifying the visibility curve at spatial frequencies lower or higher than those measured. Adding detailed structured (wiggles) to the visibility curve has remarkably little effect. The data from 2003 for R Leo is one of the most poorly fit, from a χ^2 standpoint. Fitting the data with a more detailed curve simply increases the sharpness at the edge of the dust shell and promotes some ringing in the final image as shown in Figure 25. The associated data curves are shown in Figures 26–28. The changed fit does not, however, introduce any fundamentally new structure. In general, the degree of smoothing chosen was to avoid negative intensities in the final images. The visibility is fairly well constrained at low spatial frequencies, and any sensible modifications result in little effect. The visibilities at high spatial frequencies are somewhat arbitrary approximations and could be slightly different than those presented. For this reason we concentrate on features that are within our range of resolution.

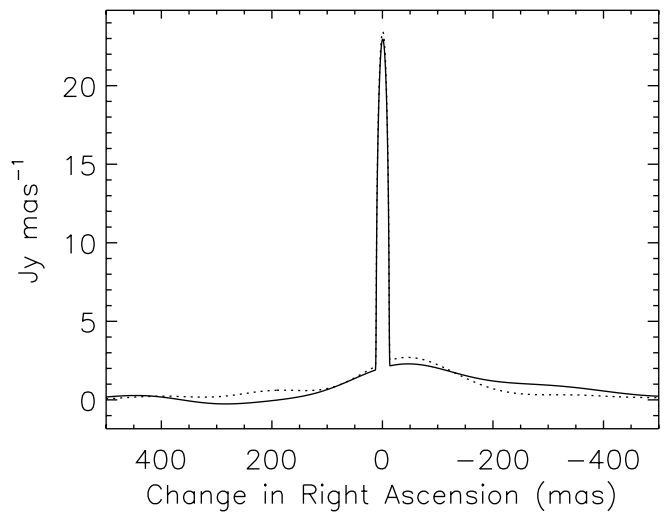

FIG. 29.—Profiles of R Aquarii using varied fits to the 2004 data. The dotted line represents the one of the smoothest possible fits, while the solid line is a fit of very high fidelity.

The closure phases present somewhat greater uncertainty as only one-third of the information is available. It is not immediately clear how sensitive structures in the image may be to changes in the curves fit to the data. Two examples where smooth, low-order analytic fits might be questioned are the data sets from 2004 for R Aqr and U Ori.

In the case of the R Aqr closure phase data there is a feature at the low-frequency end of the data where there is an upturn preceding the fall to $\sim -20^{\circ}$ where the data overlap the measurements from the previous year. Two extreme fits were used to determine which features in the images are sensitive to the fine structure of the closure phase curve and which features are more robust and must be present to maintain consistency with the data. These two cases are presented in Figures 29–32. In these figures the dotted curves are most consistent with the data but may introduce artificial structure. The solid curves are made as smooth as possible with less regard for fidelity to the original data. It is clear that the dimmer, broad features in the image change location and size, or even positivity, depending on the fit. The large lobe of intensity that is offset from the stars position, however, remains relatively constant in size and position in all these fits. Several other images were constructed using various other fits to the data, all with similar results.

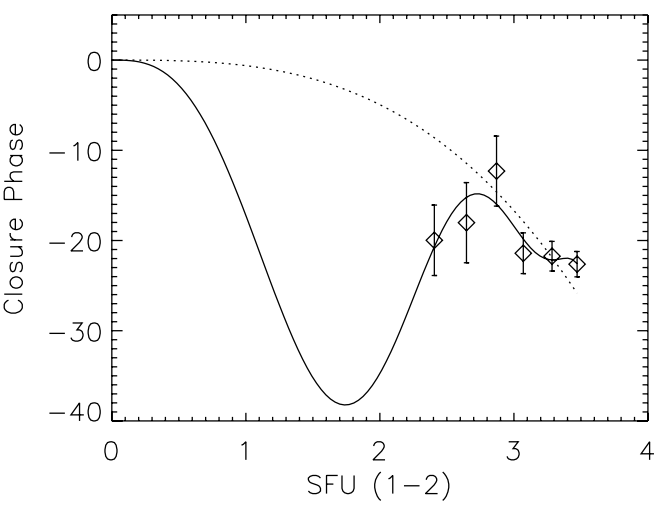

FIG. 31.—Closure phase curves for R Aquarii corresponding to the images in Fig. 29.

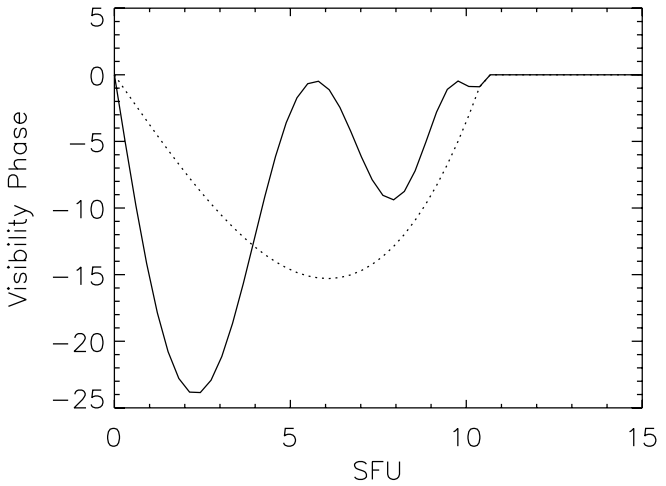

FIG. 32.—Visibility phases for R Aquarii corresponding to the closure phase curves in Fig. 31

The case of U Ori, as seen in Figure 23, clearly does not follow the assumption that the closure phase traces a smooth curve that can be analytically fit with a few terms. Here, in the 2004 data, this method largely breaks down and the image can only be regarded as a broad approximation, but is presented for comparison. As such, no conclusions are drawn directly from the images themselves but rely on features observed in the data.

Overall, the largest, "first-order" features appear to be necessary to generate an image consistent with the data. Although these features may be slightly distorted due to changes in position angle with frequency, their general size and position appear reasonably robust. Certain features, such as elongated and asymmetric hot spots, would result in rapid changes in profile with position angle and would make smooth fits to the data difficult. Most of the data sets show no indications of such complicating features, although such a feature may provide a possible explanation for the anomaly in the U Ori data.

6. CONCLUSIONS

The observations presented reveal a variety of image profiles among these six Miras. The asymmetries observed are striking and vary in character from one star to the next. Overall, the character of the asymmetry in the intensity distributions of the stars and surrounding material seems to suggest (1) stars that emit material that is accreted by a small companion have lobes of intensity offset from the star's position; (2) stars that may be asymmetric and illuminate the dust around them in an asymmetric fashion, or may emit dust asymmetrically; and (3) stars that are themselves symmetric and emit dust symmetrically.

The presence of a companion is a straightforward way of accounting for the asymmetry in the cases of R Aqr and CIT 3 and seems to be a likely, although somewhat speculative, explanation. While the existence of a companion cannot be made certain from these measurements alone, the suggestion of a companion in one case, R Aqr, may allow such profiles to aid in the search for others by examining the asymmetry of future sources. This could be particularly useful since a companion is not always readily apparent.

χ Cyg and W Aql are more puzzling, as there is no obvious and well-understood means of generating the observed asymmetries. Either asymmetric emission of material or uneven illumination of the dust may be the cause of the asymmetric profiles observed. If this is the case, it could help to account for the difficulty in modeling these complex systems with symmetric radiative transfer models. In the future, with the use of longer baselines, ISI measurements will be able to examine the asymmetries of the stars themselves. Information on the asymmetries in the photospheres of stars such as χ Cyg and W Aql may provide important clues to their dynamics and evolution. The other stars, R Leo and U Ori, have approximately symmetric distributions of intensity surrounding them. In the case of U Ori further measurements would help to determine whether the large closure phase observed in the 2004 data represents a significant and genuine feature in the dust surrounding the star.

Inspection of the collection of profiles and visibility curves presented shows that both multiple dust shells, and asymmetries in the dust and/or stars may be common among Miras. Also, it is apparent that these stars may change significantly from cycle to cycle not only in intensity but also in the distribution of dust around the stars. Continued observation of the distributions of material around such stars combined with new data on the asymmetries of the stars themselves will help to further our understanding.

This research has been helpfully supported by the Office of Naval Research, by the National Research Foundation, by NASA, and by the Gordon and Betty Moore Foundation. It has made use of the SIMBAD database and AAVSO. The authors would like to thank Ed Wishnow for his comments and suggestions, and Roger Griffith for his assistance with observations as well as in the operation and maintenance of the ISI.

REFERENCES

Baldwin, J. E., Haniff, C. A., Mackay, C. D., & Warner, P. J. 1986, Nature, 320, 595
Bowers, P. F., & Johnston, K. J. 1988, ApJ, 330, 339
Burgarella, D., Vogel, M., & Paresce, F. 1992, A&A, 262, 83
Danchi, W. C., Bester M., Degiacomi, C. G., Greenhill, L. J., & Townes, C. H. 1994, AJ, 107, 1469
Groenewegen, M. A. T. 1996, A&A, 305, L61
Hale, D. D. S. et al. 2000, ApJ, 537, 998
———. 2003, Proc. SPIE, 4838, 387
———. 2004, Proc. SPIE, 5491, 490
Haniff, C. A., Scholz, M., & Tuthill, P. G. 1995, MNRAS, 276, 640
Hege, E. K. et al. 1991, ApJ, 381, 543
Henney, W. J., & Dyson, J. E. 1992, A&A, 261, 301
Hinkle, K. H., Wilson, T. D., Scharlach, W. W. G., & Fekel, F. C. 1989, AJ, 98, 1820
Hofmann, K.-H., Balega, Y., Blöcker, T., & Weigelt, G. 2001a, A&A, 379, 529
———. 2001b, A&A, 376, 518
Hollis, J. M. et al. 1999, ApJ, 522, 297
———. 1997, ApJ, 490, 302
Jura, M., & Kanane, C. 1999, ApJ, 521, 302
Kellog, E. et al. 2001, ApJ, 563, L151
Kenyon, S. J., Fernandez-Castro, T., & Stencel, R. E. 1988, AJ, 95, 1817
Knapp, G. R., & Morris, M. 1985, ApJ, 292, 640
Lattanzi, M. G., Munari, U., Whitelock, P. A., & Feast, M. W. 1997, ApJ, 485, 328
Lipman, E. et al. 2000, ApJ, 532, 467
Loup, C., Forveille, T., Omont, A., & Paul, J. F. 1993, A&AS, 99, 291
Marengo, M. et al. 1999, A&A, 348, 501
Michalitsianos, A. G. et al. 1988, AJ, 95, 1478
Mondal, S., & Chandrasekhar, T. 2004, MNRAS, 348, 1332
Neri, R. et al. 1998, A&AS, 130, 1
Ragland, S., et al., 2006, ApJ, in press (astro-ph/0607156)
Richichi, A., & Calamai, C. 2003, A&A, 399, 275
Schuller, P. et al. 2004, A&A, 418, 151

Sloan, G. C., & Price, S. D. 1998, ApJS, 119, 141
Smith, B. J. et al. 2002, AJ, 123, 948
Sudol, J. J. et al. 1999, AJ, 117, 1609
Tevousjan, S. et al. 2004, ApJ, 611, 466
Tuthill, P. G. et al. 1998, Proc. SPIE, 3350, 839
———. et al. 1999, MNRAS, 306, 353
Tuthill, P. G. et al. 2000, ApJ, 534, 907
Vinkovic, D. et al. 2004, MNRAS, 352, 852
Wang, X.-H., & Chen, P.-S. 2002, A&A, 387, 129
Weiner, J. 2003, ApJ, 589, 976
Wolfire, M. G., & Cassinelli J. P. 1986, ApJ, 310, 207
Young, A. A. et al. 2000, MNRAS, 318, 381